SLAC-PUB-6513
May 1994
(E)

MEASURING A_b WITH POLARIZED BEAMS AT SLC *

The SLD Collaboration **
Stanford Linear Acclelerator Center
Stanford University, Stanford, CA 94309

Represented by

Thomas R. Junk
Department of Physics
Stanford University, Stanford, CA 94305

ABSTRACT

We present the first direct measurement of the left-right asymmetry of b-quarks from the decay of Z^0 bosons produced in the annihilation of longitudinally polarized electrons and unpolarized positrons in the SLD at the SLC. Two complementary techniques are presented: I) $Z^0 \to b\bar{b}$ decays are tagged using track impact parameters measured with a CCD-based vertex detector with $b - \bar{b}$ discrimination provided by momentum-weighted track charge; II) Semileptonic b-decays are tagged using high (P, P_T) muons and electrons with $b - \bar{b}$ discrimination provided by the lepton charge. In our 1993 sample of ~50,000 Z^0 decays having a luminosity-weighted average e^- polarization of $(62.6 \pm 1.2)\%$, we find the following preliminary results: $A_b(\text{track charge}) = 1.01 \pm 0.12(stat) \pm 0.14(sys)$, $A_b(\text{muons}) = 0.94 \pm 0.25(stat) \pm 0.11(sys)$, and $A_b(\text{electrons}) = 0.99 \pm 0.27(stat) \pm 0.19(sys)$.

Presented at the XXIXth Rencontres de Moriond:
Electroweak Interactions and Unified Theories
Meribel, France, March 12-19, 1994

*Work supported by the U.S. Department of Energy under Contract DE-AC03-76SF00515
**List of authors follows References.

1. Introduction

Measurements of the fermion asymmetries at the Z^0 provide direct probes of the parity violating parameters $A_f = 2v_f a_f/(v_f^2 + a_f^2)$ and hence provide a sensitive test of Standard Model predictions. Numerical values of A_f and their dependence on $\sin^2\theta_W$ have been calculated[1] and are summarized in Table 1.

$A_{e,\mu,\tau} = 0.16$	$\frac{\partial A_{e,\mu,\tau}}{\partial \sin^2\theta_W} = -7.85$
$A_{u,c} = 0.67$	$\frac{\partial A_{u,c}}{\partial \sin^2\theta_W} = -3.45$
$A_{d,s,b} = 0.94$	$\frac{\partial A_{d,s,b}}{\partial \sin^2\theta_W} = -0.63$

Table 1. Standard Model values of A_f for various fermions at the Z^0 pole for $\sin^2\theta_W = 0.230$.

The weak dependence of A_b on $\sin^2\theta_W$ and on initial state radiation makes it sensitive to an independent set of radiative corrections from those probed with A_e measurements. The strongest sensitivity of A_b to physics beyond the standard model arises from vertex loop corrections[2,3]. In the case of extensions containing two Higgs doublets, where $\tan\beta$ is defined as the ratio of their vacuum expectation values, A_b is affected by as much as 1% for large $\tan\beta$.

A common observable measured in experiments with unpolarized beams is the forward-backward asymmetry of b-quarks, A_{FB}^b. At tree level, $A_{FB}^b = \frac{3}{4}A_e A_b$. Longitudinal polarization of the electron beam, however, allows for direct measurement of A_b. At tree level, the differential cross section for b-quark production can be expresed in terms of θ, the angle of the b-quark relative to the electron beam, and the electron polarization P_e:

$$\frac{d\sigma_b}{d\cos\theta} \propto (1 - P_e A_e)(1 + \cos^2\theta) + 2(A_e - P_e)A_b \cos\theta. \tag{1}$$

The polarized asymmetry $\tilde{A}_{FB}^b$ isolates the A_b contribution by taking advantage of the separate helicity states. As a function of $\cos\theta$:

$$\tilde{A}_{FB}^b(\cos\theta) = \frac{\left\{\left.\frac{d\sigma_L^b}{d\cos\theta}\right|_{\cos\theta} - \left.\frac{d\sigma_L^b}{d\cos\theta}\right|_{-\cos\theta}\right\} - \left\{\left.\frac{d\sigma_R^b}{d\cos\theta}\right|_{\cos\theta} - \left.\frac{d\sigma_R^b}{d\cos\theta}\right|_{-\cos\theta}\right\}}{\left\{\left.\frac{d\sigma_L^b}{d\cos\theta}\right|_{\cos\theta} + \left.\frac{d\sigma_L^b}{d\cos\theta}\right|_{-\cos\theta}\right\} + \left\{\left.\frac{d\sigma_R^b}{d\cos\theta}\right|_{\cos\theta} + \left.\frac{d\sigma_R^b}{d\cos\theta}\right|_{-\cos\theta}\right\}}, \tag{2}$$

where L (R) refer to left (right) incident electron helicity, with $P_e < 0$ ($P_e > 0$). Combining eqations (1) and (2), one obtains the left-right forward-backward asymmetry of b-quark production as a function of $\cos\theta$:

$$\tilde{A}_{FB}^b(\cos\theta) = P_e A_b \frac{2\cos\theta}{1 + \cos^2\theta}. \tag{3}$$

We present here preliminary measurements of A_b from a sample of 50,000 Z^0 decays observed at $\sqrt{s} = 91.26$ GeV/c^2, with an average longitudinal electron polarization of (62.6±1.2)%. Two techniques are presented: impact-parameter tagged b-events signed with momentum-weighted track charge, and high (P, P_T) lepton tagged and signed b-events. These two approaches have independent systematic errors.

2. SLD Detector

The SLAC Large Detector[4] (SLD) analyzes the decays of Z^0 bosons produced in e^+e^- collisions at the SLC. The analysis presented here takes advantage of two tracking components, the Central Drift Chamber (CDC) and the Silicon Vertex Detector[5] (VXD), and two calorimetric components, the Liquid Argon Calorimeter[6] (LAC), and the Warm Iron Calorimeter[7] (WIC).

The CDC provides the main charged particle tracking for the SLD and consists of 80 layers of sense wires, 48 of which are stereo layers, in an axial magnetic field of 0.6 T. Tracks with polar angle $|\cos\theta| < 0.71$ traverse all 80 layers, with good reconstruction extending to $|\cos\theta| < 0.80$. The momentum resolution of the CDC is

$(\delta P_\perp/P_\perp)^2 = (.01)^2 + (.0026 P_\perp)^2$, with $P_\perp$ in GeV/c. The VXD provides precise position measurements of charged tracks near the interaction point, important for impact-parameter tagging of $Z^0 \to b\bar{b}$. It consists of 480 silicon CCD chips with a total of 120 million 22x22 μm pixels. Charge division between neighboring pixels affords an intrinsic position resolution of less than 6 μm. The CCD chips are arranged in four layers, ranging from 29.5 mm to 41.5 mm in radius. Track acceptance for the VXD extends to $|\cos\theta| < 0.75$.

The LAC measures the energies of decay products of the Z^0 and is used for electron identification in the lepton analysis. The LAC consists of a barrel and two endcap systems, with similar absorber structures. The LAC is segmented into two layers of 33x33 mr^2 projective towers in the electromagnetic section (EM), and two layers of 66x66 mrad^2 projective towers behind them in the hadronic section (HAD). The two EM layers are 6 and 15 radiation lengths thick, and the two HAD layers are each one interaction length thick. The 0.25λ solenoidal coil lies radially outside the LAC, and extends to the end of the LAC barrel section.

The WIC provides muon identification in the lepton analysis. The WIC consists of 14 layers of 2" steel plates instrumented with 18 layers of plastic limited-streamer tubes. The tubes, parallel to the beam and operated in limited streamer mode, provide 0.4x2.0 cm position resolution for ionizing particles.

The polarization of the electron beam is continuously measured with a Compton polarimeter[8] located downstream from the interaction point. Polarization measurements taken close in time to each Z^0 decay are averaged to form a luminosity-weighted polarization with negligible statistical error. The value obtained is $\langle P_e \rangle_{\mathcal{L}} = (62.6 \pm 1.2)\%$, where the systematic error results from polarimeter calibration and chromatic effects in the SLC electron arc[9].

3. Track-Charge Analysis

3.1 Event Selection and Tag

Hadronic Z^0 decays are selected by requiring that at least 7 well-reconstructed tracks ($|\cos\theta| < 0.80$) carry a large visible energy $E_{vis} > 18$ GeV/c. The dominant contribution to the residual background, $Z^0 \to \tau\bar{\tau}$ events, is estimated to be less than 0.2% of the sample.

Details of the impact parameter b-tag are given in ref. 11. Briefly, $Z^0 \to b\bar{b}$ events are tagged by requiring at least 3 tracks in the event to have two-dimensional impact parameters more than $+3\sigma$ distant from the SLC beam spot. The impact parameters are signed with respect to the nearest jet axis as determined by the JADE[10] algorithm with $y_{cut} = 0.02$, using charged tracks as input. We tag 4893 events, with an estimated efficiency of 65% and purity of 87%, with most of the contamination contributed by $Z^0 \to c\bar{c}$ decays. Figure 1 shows the dependence of the tagging fraction on the thrust axis, with a Monte Carlo estimate of the light-quark background. The thrust axis is determined using energy deposition in the LAC.

3.2 Asymmetry Measurement

For each tagged event, the momentum-weighted track-charge Q_p is calculated:

$$Q_p = \sum_{tracks} Q_i |\vec{p}_i \cdot \hat{t}|^\kappa \mathrm{sgn}(\vec{p}_i \cdot \hat{t}), \tag{4}$$

where $\hat{t}$ is a unit vector in the direction of the LAC thrust axis, and $\kappa = 0.5$ to maximize the correct-sign probability. The thrust axis is then signed to make Q_p negative, providing the best estimate of the b quark direction. Figure 2 shows the distribution of Q_p and the Monte-Carlo simulation. Figure 3 shows the signed

$\cos\theta_T$ distribution for both helicities of the incident electron beam.

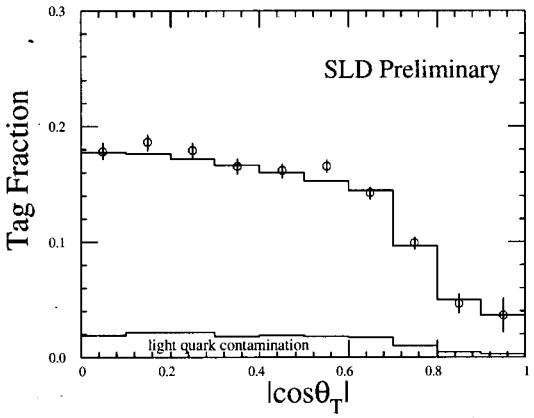

Figure 1. Impact-parameter tagging fraction as a function of $|\cos\theta_T|$. The histogram shows a Monte-Carlo simulation with light-quark contamination.

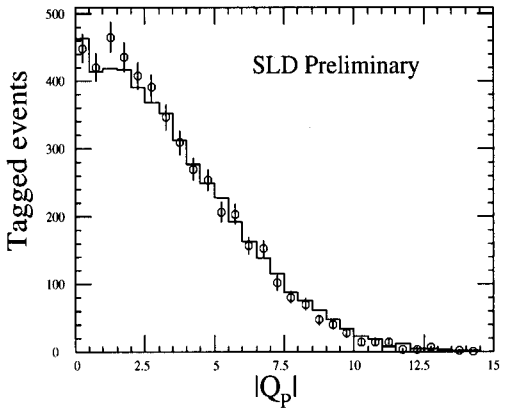

Figure 2. Momentum-weighted charge distribution for data and Monte Carlo, for $\kappa = 0.5$.

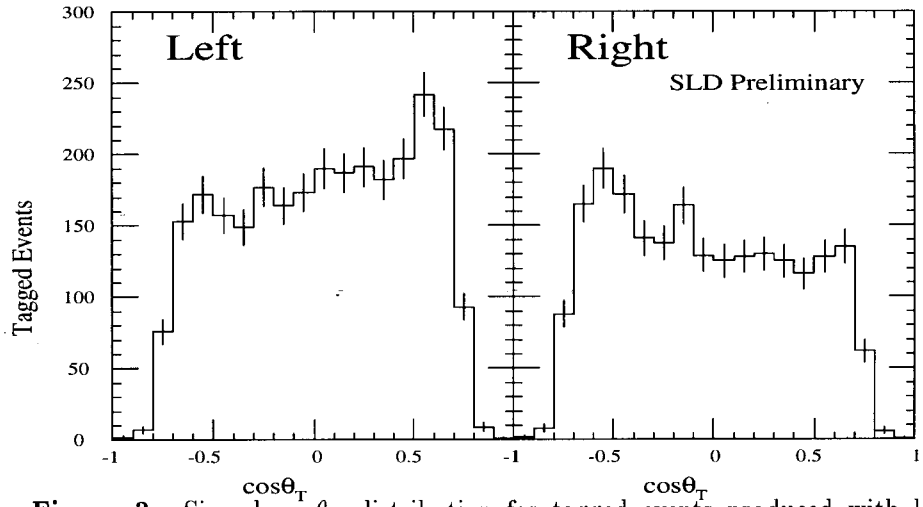

Figure 3. Signed $\cos\theta_T$ distribution for tagged events produced with left- and right-handed beams, illustrating the significant effect of polarization on the forward-backward asymmetry.

To determine A_b, the double asymmetry $\tilde{A}_{FB}(|\cos\theta_T|)$ is formed for each bin in $|\cos\theta_T|$. A small correction is applied to account for light-quark contamination, as estimated from Monte Carlo, in proportion to each flavor's asymmetry and contribution to the tag.

Corrections for asymmetry dilution due to mis-signing and smearing the thrust axis are applied by estimating in each bin of $|\cos\theta|$ the quantity ζ, the asymmetry expected if $P_e A_b$ were equal to 1.

$$\zeta(|\cos\theta_T|) = \langle \frac{2\cos\theta_b}{1+\cos^2\theta_b}(1 - \Delta_{QCD}(|\cos\theta_b|)) \rangle \tag{5}$$

where $\cos\theta_b$ is the parent quark direction and the average is taken over Monte Carlo events that reconstruct at $\cos\theta_T$. The estimated fraction of correctly signed events averages $\sim 70\%$ over accepted angles. A small ($\sim 3\%$) first-order QCD correction[12,13] $\Delta_{QCD}(|\cos\theta_b|)$ is applied to the parent asymmetry function.

With this definition, $P_e A_b$ is the slope of a linear fit to a plot of $\tilde{A}_{FB}(|\cos\theta_T|)$ versus $\zeta(|\cos\theta_T|)$, constrained to go through zero. This plot is shown in Figure 4. The fit is restricted to events in the region $|\cos\theta_T| < 0.7$, where the tracking is best modeled.

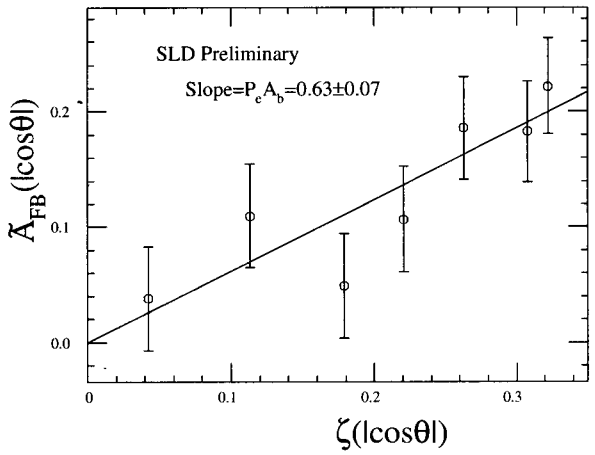

Figure 4. The observed asymmetry $\tilde{A}_{FB}(|\cos\theta_T|)$, corrected for light quark contamination, plotted against the expected asymmetry for $P_e A_b = 1.0$, $\zeta(|\cos\theta_T|)$, for each bin of $|\cos\theta_T|$. The slope yields $P_e A_b$.

CONTRIBUTION	ERROR (%)
Physics Contributions	
B-Decay Model	10
b Fragmentation	2
$B - \overline{B}$ Mixing	1
Light-Quark Asymmetry	4
Polarization	2
Detector and Tag Modeling	
Tracking Efficiency	4
Thrust Axis Resolution	2
Light-Quark Contamination	2
MC Statistics	5
TOTAL	14

Table 2. Relative systematic errors on A_b for the track-charge analysis.

3.3 Track-Charge Systematic Errors

The largest systematic errors of the track-charge technique come from uncertainties in the simulation of Q_p, where the largest contributions arise from uncertainties in the parameters of the SLD B decay model. The effect of varying the the b-fragmentation function shape and mean value is small because the fragmentation tracks contribute little to Q_p. Mixing is a small error because the B^0 and the B_s^0 have relatively small $\langle Q_p \rangle$. Table 2 summarizes our estimates of these errors, which are combined in quadrature for our preliminary result:

$$A_b(\text{track charge}) = 1.01 \pm 0.12(stat) \pm 0.14(sys) \tag{6}$$

Comparing the track-charge assignment of opposing hemispheres allows confirmation, independent of the value of $P_e A_b$, that the charge flow is well simulated by the Monte Carlo. The fraction of tagged events with hemispheres agreeing on the direction of the b quark is denoted P_{agree}, with $P_{disagree} = 1 - P_{agree}$. The ratio $(P_{agree} - P_{disagree})/(P_{agree} + P_{disagree})$ is found to be 0.0934 ± 0.0071 in data and 0.103 ± 0.0035 in the Monte Carlo, indicating that the charge flow is properly modeled. One may also compare the widths of two hemisphere distributions: the sum of Q_p from each hemisphere, and the difference of Q_p in each hemisphere on an event-by-event basis. The asymmetry dilution is directly given by $\text{erf}(\sqrt{\frac{\sigma_{diff}}{\sigma_{sum}} - 1})$. Hemisphere checks of the modeling are sensitive to correlations between the hemispheres and work is in progress to improve the understanding of such correlations.

4. Lepton Analysis

The second analysis uses leptons to tag $Z^0 \to b\bar{b}$ events and to sign the b-quark. This technique has smaller systematic uncertainties than the track-charge analysis, but it has less statistical power due to the small B semileptonic branching fraction.

4.1 Lepton Identification

Muons are identified in the WIC by extrapolating tracks measured in the CDC through the LAC and solenoid coil while properly accounting for energy loss and multiple scattering. Tracks are required to lie within $|\cos\theta| < 0.70$. The LAC imposes a momentum cutoff of 2.0 GeV/c at normal incidence. Tracks penetrating the LAC and coil

are linked to candidate hits in the 18 layers of the WIC, and tracks are required to penetrate the WIC fully. For muons with momenta greater than 3.0 GeV/c the efficiency of this procedure is 85%, while the pion misidentification probability is estimated to be less than 0.15%.

Electrons are identified in the SLD by extrapolating charged tracks to the barrel LAC. We require that the total energy collected in the electromagnetic sections in a 3x3 array of towers centered on the extrapolated track be close to the track momentum, $-2\sigma < [(EM\text{energy})/p_{track}] < 3\sigma$, where σ is the expected error in the ratio. We also require that more than 25% of the EM energy be deposited in the first EM layer. Finally, we require that there be less than 0.24 GeV/c^2 deposited in the single hadronic tower to which the track extrapolates. The estimated efficiency for identifying electrons in hadronic Z^0 events is 70% for $|\cos\theta| < 0.7$. The misidentification rate for isolated pions is 2% at a mometum of 1 GeV/c, diminishing to 1% for momenta greater than 4 GeV/c.

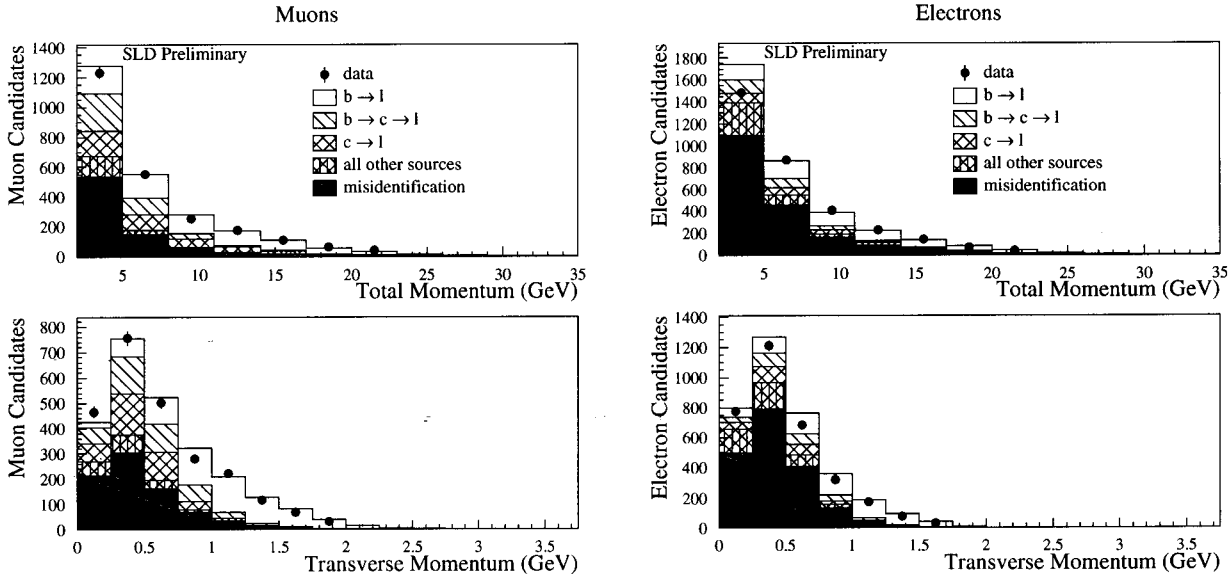

Figure 6. Spectra of tagged lepton candidates projected onto P and P_T with Monte Carlo estimations of contributions from signal and background sources.

4.2 Asymmetry Measurement

Electrons and muons with high momentum P and high transverse momentum P_T relative to the nearest jet axis are selected by an elliptical cut of $(\frac{P}{16GeV})^2 + (\frac{P_T}{1.2GeV})^2 > 1$. A total of 560 muon candidates and 454 electron candidates are selected, and they come predominantly from prompt B decay, as shown in figure 6. Table 3 describes by source the contributions of leptons in this sample, as estimated by Monte-Carlo. The relative magnitudes of these contributions are used to derive the analyzing power for the lepton asymmetry analyses.

SOURCE	Asymmetry	Muon Fraction	Electron Fraction
$b \to l$	$+(1-2\chi)A_b$	0.723 ± 0.015	0.610 ± 0.024
$b \to \bar{c} \to l$	$+(1-2\chi)A_b$	0.005 ± 0.001	0.002 ± 0.001
$b \to c \to \bar{l}$	$-(1-2\chi)A_b$	0.050 ± 0.004	0.049 ± 0.007
$c \to \bar{l}$	$A_c = -0.72A_b$	0.084 ± 0.005	0.052 ± 0.007
light hadron decay	$\langle A_{back} \rangle$	0.016 ± 0.002	0.046 ± 0.007
misidentification	$\langle A_{back} \rangle$	0.122 ± 0.006	0.241 ± 0.015

Table 3. Sources of leptons in the high-(P, P_T) sample.

The left-right forward-backward asymmetry $\tilde{A}_{FB}(\cos\theta)$ for the electrons and muons is formed as in the track-charge analysis, where $\cos\theta_b$ is approximated by the direction of the LAC jet nearest the lepton, rather than the

thrust axis. The charge of the lepton provides $b - \bar{b}$ discrimination, determining the appropriate sign of $\cos\theta$. To estimate the asymmetry dilution due to $B\overline{B}$ mixing, we use the LEP average $\chi = 0.115 \pm 0.011$ as measured in dilepton-tagged events[14]. Table 4 summarizes systematic errors in modeling the asymmetry dilutions for both lepton analyses. When adjusted for the electron polarization, the resulting preliminary measurements of A_b are:

$$A_b(muons) = 0.94 \pm 0.25 \pm 0.11 \tag{7}$$

$$A_b(electrons) = 0.99 \pm 0.27 \pm 0.19 \tag{8}$$

SOURCE	Muons	Electrons
Tracking efficiency	0.03	0.02
Jet axis simulation	0.04	0.04
Background level	0.01	0.07
B Mixing	0.03	0.03
Monte Carlo statistics	0.02	0.03
$\Gamma(Z^0 \to b\bar{b})$	0.01	0.02
$\Gamma(Z^0 \to c\bar{c})$	0.02	0.01
$B^0, B^{\pm}$ lepton spectrum	0.06	0.09
B_s lepton spectrum	0.06	0.07
Λ_b lepton spectrum	0.01	0.01
c fragmentation	0.03	0.03
b fragmentation	0.01	0.04
A_c	0.02	0.02
Background asymmetry	0.02	0.10
Polarization	0.02	0.02
Second-order QCD corrections	0.01	0.01
TOTAL	0.11	0.19

Table 4. Relative systematic errors on A_b for the lepton analyses.

References

1. A. Blondel, B.W. Lynn, F.M. Renard, and C. Verzegnassi, *Nuclear Physics* **B304** (1988) p. 438-450.
2. M. Boulware and D. Finnell, *Physical Review* **D44** (1991) p. 2054-2063.
3. D. Comelli, C. Verzegnassi, and F.M. Renard, "Information and Discrimination from b Quark Production on Z Resonance" HEP-PH-9402305 (1994)
4. *SLD Design Report*, SLAC Report SLAC-273 (1984)
5. G.D. Agnew *et al.*, *Proceedings of the XXVI Int'l Conf. on High Energy Physics, Dallas* (1992).
6. D. Axen *et al.*, *Nucl. Instrum. Methods* **A328** (1993) p. 472-494.
7. A. C. Benvenuti *et al.*, *Nucl. Instrum. Methods* **A290** (1990) p. 353.
8. C. Y. Prescott, SLAC-PUB-6355 (1993).
   See also D. Calloway *et al.*, SLAC-PUB-6423 (in preparation), to be submitted to *Nucl. Instrum. Methods.*
9. M. Woods *et al.*, SLAC-PUB-6493 (1994).
   See also K. Abe *et al.*, SLAC-PUB-6456 (1994), submitted to *Phys. Rev. Lett.*
10. JADE Collaboration, *Z. Phys.* **C33** (1986) p. 23.
11. K. Abe *et al.*, SLAC-PUB 6292 (1993).
12. A. Djouadi, J.H. Kühn, and P.M. Zerwas, *Z. Phys* **C46** (1990) p. 411-417.
13. G. Altarelli and B. Lampe, *Nucl. Phys.* **B391** (1993) p. 3-22.
14. LEP Electroweak Working Group, CERN/PPE/93-157 (1993)

The SLD Collaboration

K. Abe,[27] I. Abt,[13] W.W. Ash,[25]† D. Aston,[25] N. Bacchetta,[20] K.G. Baird,[23] C. Baltay,[31] H.R. Band,[30] M.B. Barakat,[31] G. Baranko,[9] O. Bardon,[16] T. Barklow,[25] A.O. Bazarko,[10] R. Ben-David,[31] A.C. Benvenuti,[2] T. Bienz,[25] G.M. Bilei,[21] D. Bisello,[20] G. Blaylock,[7] J.R. Bogart,[25] T. Bolton,[10] G.R. Bower,[25] J.E. Brau,[19] M. Breidenbach,[25] W.M. Bugg,[26] D. Burke,[25] T.H. Burnett,[29] P.N. Burrows,[16] W. Busza,[16] A. Calcaterra,[12] D.O. Caldwell,[6] D. Calloway,[25] B. Camanzi,[11] M. Carpinelli,[22] R. Cassell,[25] R. Castaldi,[22][a] A. Castro,[20] M. Cavalli-Sforza,[7] E. Church,[29] H.O. Cohn,[26] J.A. Coller,[3] V. Cook,[29] R. Cotton,[4] R.F. Cowan,[16] D.G. Coyne,[7] A. D'Oliveira,[8] C.J.S. Damerell,[24] S. Dasu,[25] F.J. Decker,[25] R. De Sangro,[12] P. De Simone,[12] S. De Simone,[12] R. Dell'Orso,[22] Y.C. Du,[26] R. Dubois,[25] J.E. Duboscq,[6] B.I. Eisenstein,[13] R. Elia,[25] P. Emma,[25] C. Fan ,[9] M.J. Fero,[16] R. Frey,[19] K. Furuno,[19] E.L. Garwin,[25] T. Gillman,[24] G. Gladding,[13] S. Gonzalez,[16] G.D. Hallewell,[25] E.L. Hart,[26] Y. Hasegawa,[27] S. Hedges,[4] S.S. Hertzbach,[17] M.D. Hildreth,[25] D.G. Hitlin,[5] J. Huber,[19] M.E. Huffer,[25] E.W. Hughes,[25] H. Hwang,[19] Y. Iwasaki,[27] J.M. Izen,[13] P. Jacques,[23] J. Jaros,[25] A.S. Johnson,[3] J.R. Johnson,[30] R.A. Johnson,[8] T. Junk,[25] R. Kajikawa,[18] M. Kalelkar,[23] I. Karliner,[13] H. Kawahara,[25] M.H. Kelsey,[5] H.W. Kendall,[16] M.E. King,[25] R. King,[25] R.R. Kofler,[17] N.M. Krishna,[9] R.S. Kroeger,[26] Y. Kwon,[25] J.F. Labs,[25] M. Langston,[19] A. Lath,[16] J.A. Lauber,[9] D.W.G. Leith,[25] T. Limberg,[25] X. Liu ,[7] M. Loreti,[20] A. Lu ,[6] H.L. Lynch,[25] J. Ma ,[29] G. Mancinelli,[21] S. Manly,[31] G. Mantovani,[21] T.W. Markiewicz,[25] T. Maruyama,[25] H. Masuda,[25] E. Mazzucato,[11] J.F. McGowan,[13] A.K. McKemey,[4] B.T. Meadows,[8] R. Messner,[25] P.M. Mockett,[29] K.C. Moffeit,[25] B. Mours,[25] G. Müller,[25] D. Muller,[25] T. Nagamine,[25] U. Nauenberg,[9] H. Neal,[25] M. Nussbaum,[8] L.S. Osborne,[16] R.S. Panvini,[28] H. Park,[19] T.J. Pavel,[25] I. Peruzzi,[12][b] L. Pescara,[20] M. Piccolo,[12] L. Piemontese,[11] E. Pieroni,[22] K.T. Pitts,[19] R.J. Plano,[23] R. Prepost,[30] C.Y. Prescott,[25] G.D. Punkar,[25] J. Quigley,[16] B.N. Ratcliff,[25] T.W. Reeves,[28] P.E. Rensing,[25] L.S. Rochester,[25] J.E. Rothberg,[29] P.C. Rowson,[10] J.J. Russell,[25] O.H. Saxton,[25] T. Schalk,[7] R.H. Schindler,[25] U. Schneekloth,[16] D. Schultz,[25] B.A. Schumm,[15] A. Seiden,[7] S. Sen ,[31] M.H. Shaevitz,[10] J.T. Shank,[3] G. Shapiro,[15] D.J. Sherden,[25] C. Simopoulos,[25] S.R. Smith,[25] J.A. Snyder,[31] M.D. Sokoloff,[8] P. Stamer,[23] H. Steiner,[15] R. Steiner,[1] M.G. Strauss,[17] D. Su,[25] F. Suekane,[27] A. Sugiyama,[18] S. Suzuki,[18] M. Swartz,[25] A. Szumilo,[29] T. Takahashi,[25] F.E. Taylor,[16] E. Torrence,[16] J.D. Turk,[31] T. Usher,[25] J. Va'Vra,[25] C. Vannini,[22] E. Vella,[25] J.P. Venuti,[28] P.G. Verdini,[22] S.R. Wagner,[25] A.P. Waite,[25] S.J. Watts,[4] A.W. Weidemann,[26] J.S. Whitaker,[3] S.L. White,[26] F.J. Wickens,[24] D.A. Williams,[7] D.C. Williams,[16] S.H. Williams,[25] S. Willocq,[31] R.J. Wilson,[3] W.J. Wisniewski,[5] M. Woods,[25] G.B. Word,[23] J. Wyss,[20] R.K. Yamamoto,[16] J.M. Yamartino,[16] S.J. Yellin,[6] C.C. Young,[25] H. Yuta,[27] G. Zapalac,[30] R.W. Zdarko,[25] C. Zeitlin,[19] and J. Zhou,[19]

[1]Adelphi University, Garden City, New York 11530
[2]INFN Sezione di Bologna, I-40126 Bologna, Italy
[3]Boston University, Boston, Massachusetts 02215
[4]Brunel University, Uxbridge, Middlesex UB8 3PH, United Kingdom
[5]California Institute of Technology, Pasadena, California 91125
[6]University of California at Santa Barbara, Santa Barbara, California 93106
[7]University of California at Santa Cruz, Santa Cruz, California 95064
[8]University of Cincinnati, Cincinnati, Ohio 45221
[9]University of Colorado, Boulder, Colorado 80309
[10]Columbia University, New York, New York 10027

[11]INFN Sezione di Ferrara and Università di Ferrara, I-44100 Ferrara, Italy
[12]INFN Lab. Nazionali di Frascati, I-00044 Frascati, Italy
[13]University of Illinois, Urbana, Illinois 61801
[14]KEK National Laboratory, Tsukuba-shi, Ibaraki-ken 305 Japan
[15]Lawrence Berkeley Laboratory, University of California, Berkeley, California 94720
[16]Massachusetts Institute of Technology, Cambridge, Massachusetts 02139
[17]University of Massachusetts, Amherst, Massachusetts 01003
[18]Nagoya University, Chikusa-ku, Nagoya 464 Japan
[19]University of Oregon, Eugene, Oregon 97403
[20]INFN Sezione di Padova and Università di Padova, I-35100 Padova, Italy
[21]INFN Sezione di Perugia and Università di Perugia, I-06100 Perugia, Italy
[22]INFN Sezione di Pisa and Università di Pisa, I-56100 Pisa, Italy
[23]Rutgers University, Piscataway, New Jersey 08855
[24]Rutherford Appleton Laboratory, Chilton, Didcot, Oxon OX11 0QX United Kingdom
[25]Stanford Linear Accelerator Center, Stanford University, Stanford, California 94309
[26]University of Tennessee, Knoxville, Tennessee 37996
[27]Tohoku University, Sendai 980 Japan
[28]Vanderbilt University, Nashville, Tennessee 37235
[29]University of Washington, Seattle, Washington 98195
[30]University of Wisconsin, Madison, Wisconsin 53706
[31]Yale University, New Haven, Connecticut 06511
†Deceased
[a]Also at the Università di Genova
[b]Also at the Università di Perugia